OXFORD

Electroconvulsive therapy selectively enhanced feedforward connectivity from fusiform face area to amygdala in major depressive disorder

Jiaojian Wang,[1] Qiang Wei,[2] Tongjian Bai,[2] Xiaoqin Zhou,[3] Hui Sun,[4] Benjamin Becker,[1] Yanghua Tian,[2] Kai Wang,[2] and Keith Kendrick[1]

[1]Key Laboratory for NeuroInformation of the Ministry of Education, School of Life Science and Technology, University of Electronic Science and Technology of China, Chengdu 625014, China, [2]Department of Neurology, The First Hospital of Anhui Medical University, Hefei 230022, China,[3]Anhui Mental Health Center, Hefei 230022, China, and [4]Beijing Key Laboratory of Learning and Cognition, School of Education, Capital Normal University, Beijing 100048, China

Jiaojian Wang and Qiang Wei contributed equally to this work.
Correspondence should be addressed to Yanghua Tian, Department of Neurology, The First Hospital of Anhui Medical University, Hefei 230022, China. E-mail: ayfytyh @126.com.

Abstract

Electroconvulsive therapy (ECT) has been widely used to treat the major depressive disorder (MDD), especially for treatment-resistant depression. However, the neuroanatomical basis of ECT remains an open problem. In our study, we combined the voxel-based morphology (VBM), resting-state functional connectivity (RSFC) and granger causality analysis (GCA) to identify the longitudinal changes of structure and function in 23 MDD patients before and after ECT. In addition, multivariate pattern analysis using linear support vector machine (SVM) was applied to classify 23 depressed patients from 25 gender, age and education matched healthy controls. VBM analysis revealed the increased gray matter volume of left superficial amygdala after ECT. The following RSFC and GCA analyses further identified the enhanced functional connectivity between left amygdala and left fusiform face area (FFA) and effective connectivity from FFA to amygdala after ECT, respectively. Moreover, SVM-based classification achieved an accuracy of 83.33%, a sensitivity of 82.61% and a specificity of 84% by leave-one-out cross-validation. Our findings indicated that ECT may facilitate the neurogenesis of amygdala and selectively enhance the feedforward cortical–subcortical connectivity from FFA to amygdala. This study may shed new light on the pathological mechanism of MDD and may provide the neuroanatomical basis for ECT.

Key words: major depressive disorder; ECT; amygdala; fusiform face area; multivariate pattern analysis

Introduction

Major depressive disorder (MDD), which is one of the most common mental disorders, is the leading cause of disability worldwide and a major contributor to the global burden of disease (Ferrari *et al.*, 2013). With the progress of the disease, the severely depressed patients may have suicide attempt or even commit suicide. Given the slow effect of medication,

electroconvulsive therapy (ECT), which is a rapid and effective way to alleviate the disease symptoms, has been widely used to treat the severe depression patients who have not responded to multiple medication trials or who are at imminent risk of suicide (Lisanby, 2007; Kellner *et al.*, 2012). However, the neural basis of the ECT relieving symptoms of depression is still largely unknown.

There are several theories were proposed to illuminate the mechanisms of ECT (Kellner *et al.*, 2012). An increasing number of **studies** has suggested that the antidepressant effect results from ECT mediating neuroplasticity which induced increased rates of neurogenesis, synaptogenesis and glial proliferation (Madsen *et al.*, 2000; Nobler *et al.*, 2001; Santarelli *et al.*, 2003; Chen *et al.*, 2009; Piccinni *et al.*, 2009). Modern structural magnetic resonance imaging (sMRI) technique has identified the structural changes in frontal and medial temporal cortex (Dukart *et al.*, 2014; Joshi *et al.*, 2016). However, only assessing the structural changes cannot inform the abnormal functional connectivity patterns with other brain areas, which actually determines the functions of a brain area (Passingham *et al.*, 2002). Recently, resting-state functional connectivity (RSFC) analysis has been adopted to reveal the functional networks' changes after ECT. Perrin *et al.* (2012) found that the average global functional connectivity was decreased in the left dorsolateral prefrontal cortex (dlPFC) after ECT. Subsequently, Abbott *et al.* (2013) identified a significantly increased pattern of functional network connectivity between the posterior default mode network and the left dlPFC in ECT remitters compared with ECT non-remitters. The discrepancy of these findings among different studies raises the question what's the exact role of ECT on alleviating symptoms of depression.

In this study, we aimed to uncover the possible neurophysiological basis of ECT using structural and resting-state functional MRI (rs-fMRI). The sMRI was used to characterize the changes of brain gray matter volume (GMV), whereas the rs-fMRI was used to reveal the changed functional networks. rs-fMRI, which predominantly reflects the spontaneous brain functional activities related to self-initiated behavior (Fox and Raichle, 2007), could better characterize the changes of the intrinsic functional connectivity patterns. However, RSFC cannot identify the causal effects between brain areas, thus, Granger causality analysis (GCA) was additionally applied to reveal the causal interactions between brain areas. Because of the lag between hemodynamic response function (HRF) and sampling rate of fMRI data, the inhibitory and excitatory nature of neuronal clusters and the size of neuronal cluster activation can diminish the ability to correctly identify causality across the brain. However, although GCA of fMRI data is still controversial, emerging reports have demonstrated that GCA can effectively identify the directed functional interactions between brain areas (Sridharan *et al.*, 2008; Hamilton *et al.*, 2011). Finally, multivariate pattern analysis using linear support vector machine (SVM) was employed to test whether these altered neural indices can serve as biomarkers for diagnosing MDD.

Materials and methods

Participants

Twenty-three MDD patients participating in ECT treatment were recruited in the Anhui Mental Health Center in Anhui province of China. Parts of participants' fMRI data were used in a previous study (Wei *et al.*, 2014). Diagnosis of a MDD was evaluated by a trained senior psychiatrist Xiaoqin Zhou (XQZ) based on Diagnostic and Statistical Manual of Mental Disorders-IV (DSM-IV) criteria. Patients with a treatment-resistant MDD or with acute suicidal tendencies were assigned to ECT. Exclusion criteria for this study were **substance use disorder**, pregnancy, life threatening somatic disease, neurological disorders, other comorbid mental disorders, previous ECT treatment as well as MRI-contraindications. Finally, a total of 23 participants (11 males and 12 females, **range** from 18 to 55 years, mean age = 38.74 years, s.d. = 11.02; mean education level = 8.83 years, s.d. = 3.89) were enrolled in this study. All patients continued to take antidepressive medication during the course of the study (details presented in Table 1). The severity of depression was assessed using the 17-item Hamilton Rating Scale for Depression (HRSD) (Hamilton, 1960). The scale was administered 12–24 h before the first ECT and 24–72 h after the last ECT. The antidepressive ECT treatment response was evaluated using a paired two-sided *t*-test on the HRSD scores, and the threshold for significance was set at $P < 0.05$. As a reference group 25 gender, age and education matched healthy controls (HC) (12 males and 13 females, range from 26 to 51 years, mean age = 39.52 years, s.d. = 8.07; mean education level = 8.84 years, s.d. = 3.05) were included in this study. All participants were right-handed and provided written informed consent. The study was in accordance with the latest revision of the declaration of Helsinki and experimental procedures and had full ethical approval from the local ethics committees of the Anhui Medical University (**ethics committee reference number: 20140072**).

Table 1. Demographic and clinical variables

Subjects	MDD	Healthy controls	P value
Number of subjects	23	25	
Age (mean ± s.d.)	38.74 ± 11.02	39.52 ± 8.07	0.7794
Gender (male/female)	11/12	12/13	0.9904
Education level (mean ± s.d.)	8.83 ± 3.89	8.84 ± 3.05	0.9890
HRSD scores (mean ± s.d.)			
Before ECT	22.22 ± 4.74		
After ECT	3.83 ± 2.15		
Number of treatment (mean ± s.d.)	7.26 ± 2		
Age of onset (years)	33.90 ± 12.26		
Durations of illness (months)	70.35 ± 83.27		
Episodes (*n* patients)			
First	8		
Recurrence	15		
Family history (*n* patients)	2		
Medication (*n* patients)	23		
Medication-free	0		
On-medication	23		
SSRIs	7		
SNRIs	4		
SSRIs + SNRIs	1		
SSRIs + NaSSAs	1		
SSRIs + SARIs	1		
SSRIs + antipsychotics	9		

Note: A Pearson chi-squared test was used for gender comparison. Two-sample *t*-tests were used for age, education comparisons. MDD, major depressive disorder; HRSD, Hamilton Rating Scale for Depression; SSRIs, selective serotonin reuptake inhibitors; SNRIs, serotonin-norepinephrine reuptake inhibitors; NaSSAs, norepinephrine and specificity serotonergic antidepressants; SARIs, serotonin antagonist/reuptake inhibitors.

ECT procedures

Patients underwent a modified bifrontal ECT protocol using a Thymatron System IV Integrated ECT System (Somatics, Lake Bluff, IL) in the Anhui Mental Health Center. The first three ECT sessions were administered on consecutive days, and the subsequent ECT sessions were conducted every other day with a break over the weekends until patients' reached symptom remission. The initial percent energy dial was set based on the age of each participant (e.g. 50% for a 50-year-old patient). The stimulation strength can be evenly adjusted with an increment of 5% of the maximum charge. The maximum stimulus charge is ~1000 mC (millicoulomb) in our treatment strategy (Thymatron 2× instrument). If no seizure activity was detected with the initial stimulation setting, the percent energy was increased until seizure was visually observed. The ECT procedure was administered under propofol anesthesia. Succinylcholine and atropine were additionally administered to relax the musculature and suppress the secretion of glands. Seizure activity was additionally monitored via electroencephalography (Wei *et al.*, 2014).

MRI data acquisition

All MRI data were acquired on a clinical 3.0 T whole-body MRI system (Signa HDxt, GE Healthcare, Buckinghamshire, UK) at the First Affiliated Hospital of Anhui Medical University in Anhui province of China. Patients were scanned 12–24 h before the first ECT and 24–72 h after the last ECT. To determine pre-treatment neural alterations in the patients, HC were scanned once. Participants were instructed to relax and to keep their eyes closed, to remain awake and not to think of anything during the MRI acquisition. T1-weighted anatomic images were acquired in sagittal orientation with three-dimensional inversion recovery prepared fast spoiled gradient recalled sequence (repetition time/echo time ratio = 8.676/3.184 ms, inversion time 800 ms, flip angle = 8°, field of view = $256 \times 256 \, mm^2$, matrix size = 256×256, slice thickness = 1 mm, voxel size = $1 \times 1 \times 1 \, mm^3$, sections = 188). The resting-state functional images were acquired using a standard echo planar imaging (EPI) sequence (repetition time/echo time ratio = 2000/22.5 ms, 240 volumes, flip angle = 30°, 33 slices, thickness/gap = 4.0/0.6 mm, voxel size = $3.4 \times 3.4 \times 4.6 \, mm^3$, matrix size = 64×64, field of view = $220 \times 220 \, mm^2$).

VBM analyses

Voxel-based morphology (VBM) analyses were performed to determine brain structural changes before and after ECT in the MDD patients as well as to determine pre-treatment differences between patients and controls. The sMRI images were preprocessed using VBM8 toolbox (http://dbm.neuro.uni-jena.de/vbm.html) in SPM8 (Statistical Parametric Mapping software: http://www.fil.ion.ucl.ac.uk/spm). The modulated VBM8 were used to calculate the GMV and were corrected for total intracranial volume. In this study, we used the longitudinal VBM analyses of the sMRI data before and after ECT. Within-subject midway coregistration was performed to account for between-session variance. Each structural image was segmented into gray matter, white matter and cerebrospinal fluid using a fully automated algorithm within SPM8 and subsequently transformed to Montreal Neurological Institute (MNI) space using Diffeomorphic anatomical registration through exponentiated Lie algebra (DARTEL)-normalization. Next, the normalized gray matter images were smoothed for statistical analyses (Ashburner and Friston, 2000). Finally, a paired *t*-test (whole brain volume as covariant) was performed on these normalized GMV maps to determine brain regions with significant pre–post-treatment differences. Voxel-wise family wise error (FWE) correction was used for multicomparison correction to control type 1 error (P < 0.05, FWE corrected, minimum cluster size ≥ 30 voxels). To control the effects of different Gaussian smoothing kernels, we used Gaussian kernels with different full-width at half-maximum (FWHM = 4, 6, 8 and 10) to smooth the normalized gray matter images for the subsequent statistical analyses. Next, the overlap between the results obtained under different smooth kernels was reported as final result. Finally, the overlapping results from the different smoothing kernels were used as seed region for the subsequent functional connectivity analyses. For the cross-sectional comparison between pre-treatment brain structural differences between patients and controls, standard VBM procedures were employed to calculate the HC participants' GMV. Next, we extracted the mean GMV of the brain regions with changed GMV after ECT. Then, two-sample *t*-test was performed between the HC and pre-treatment of MDD patients and significant level was set at P < 0.05.

Localization of brain structural changes

To determine the exact anatomical location of significant differences in GMV, results were mapped using cytoarchitectonical maps, allowing to determine probabilistic localization within subregions of the amygdala including the superficial (SF) subregion, centromedial (CM) subregion and laterobasal (LB) subregion as provided within the Anatomy toolbox (Eickhoff *et al.*, 2005).

rs-fMRI data preprocessing

The preprocessing of the rs-fMRI data were carried out using SPM8 software. The first 10 volumes were discarded to allow for magnetization equilibrium. The slice timing for the remaining images was corrected, and images were realigned to the first volume to account for head motion. All participants showed a maximum displacement of < 3 mm and an angular motion of < 3° and thus were included in the subsequent analyses. All fMRI images were normalized to MNI EPI template and resampled at $3 \times 3 \times 3 \, mm^3$. Finally, the functional images were smoothed using a Gaussian kernel of 6 mm FWHM. Subsequently, the functional images were filtered with a temporal band-path of 0.01–0.1 Hz and six motion parameters, white matter and cerebrospinal fluid signals were regressed out. Because previous studies have shown that global mean signal regression can lead to spurious resting-state functional correlations and false inferences, particularly on the group level inference (Gotts *et al.*, 2013; Saad *et al.*, 2013), the global mean signal was not regressed during the preprocessing in this study.

RSFC analyses

To identify whether ECT changed the functional interplay of regions displaying significant GMV changes during ECT treatment, whole brain RSFC, which is defined by the Pearson correlation between the time series, was computed using clusters with significant GMV changes during treatment as seed region. To calculate the RSFC, we first resampled the brain areas identified in VBM analyses to 3 mm cubic voxels in MNI space. The Pearson correlation coefficients between the mean time series for each seed region and the mean time series for each voxel of the whole brain were next calculated for each subject and then converted to z values using Fisher's z transformation to improve normality. On the group level, each individual's z values were entered into a paired *t*-test (head motion

parameters as covariant) in a voxel-wise manner to determine the regions that showed significantly different connectivity to the seed region. Significance was determined using a cluster-level Monte Carlo simulation (5000 times) corrected threshold of $P < 0.05$ (cluster-forming threshold at voxel-level $P < 0.001$).

Meta-analysis to define FFA

To determine whether the areas showing functional changes corresponded to the fusiform face area (FFA), a meta-analytic method was used to define the anatomical location of the FFA using the BrainMap database (www.brainmap.org). For the meta-analytic approach only task-based fMRI studies in healthy participants that reported functional mapping experiments using face monitor/discrimination paradigms were included. In addition, only the experiments reported activation were included. We excluded the studies in patient population or specifically examining gender differences. No further constraints were enforced. According to these criteria, 118 articles with 394 experiments were included and the corresponding coordinate files were downloaded. Next, we performed activation likelihood estimation (ALE) in standard MNI space using, and the resultant ALE map was corrected using false discovery rate (FDR) $P < 0.01$ with minimum volume $= 200\,mm^3$. After **obtaining** the FFA, we mapped the functionally changed area to the FFA to determine the correspondence between the two regions.

GCA of ECT-induced brain functional changes

GCA was performed to further explore the causal interaction between brain areas with functional connectivity changes before and after ECT. GCA was performed using the Causal Connectivity Toolbox (Seth, 2010). We first extracted the mean time series of the brain areas determined by RSFC analyses. Then, the bivariate GCA was performed on the time series to test the causal interactions. The order of the autoregressive model used for computation of the influence measure was selected using the Bayesian information criterion and magnitudes of causal interactions were obtained. Finally, a paired t-test was performed on the magnitudes of causal interactions to identify the significantly causal influences between brain areas using a significance threshold of $P < 0.05$.

Multivariate pattern analysis using SVM

To explore whether the identified neural indices might serve as biomarkers for diagnosing MDD, a linear SVM approach within a library for SVMs (LIBSVMs) toolkit running on MATLAB (Chang and Lin, 2011) was performed. The mean regional GMV of amygdala, functional connectivity between amygdala and FFA, and effective connectivity from FFA to amygdala were used as the features for classification. We used a leave-one-out cross-validation strategy because of our limited number of samples to estimate the generalization ability of our classifier. The performance of a classifier was assessed using the classification accuracy, sensitivity and specificity based on the results of the cross-validation.

Functional characterization with BrainMap database

To determine the functional roles of the brain regions showing ECT-associated changes, a behavioral characterization using the BrainMap database was performed. The behavioral domains were determined by examining which types of tasks were significantly associated with the identified regions. The behavioral domain analysis included 5 behavioral domains and 51

behavioral subdomains. Functional characterization of the regions showing ECT-associated structural and functional changes was determined using forward inferences (Bzdok *et al.*, 2013). The significance was established using a binomial test ($P < 0.05$) corrected for multiple comparisons using FDR.

Correlation analysis

We performed correlation analysis between each subject's mean GMV, functional connectivity strength and the causal connectivity strength and the HRSD scores to further explore whether neuroimaging indices were related to changes on the symptom-level. The significance level was set at $P < 0.05$.

Results

Demographic and clinical characteristics

There were no significant differences in age ($P = 0.7794$), gender ($P = 0.9904$) and education level ($P = 0.9890$) between MDD and HC groups (Table 1). Within the group of MDD patients' depressive symptom load as assessed by the HRSD significantly decreased during the course of ECT treatment (Figure 1).

GMV changes

The VBM analyses consistently identified increased amygdala GMV following ECT in different smooth kernels (Figure 2A). The overlap of the results obtained with different smooth kernels was found to be located in the left amygdala [MNI central coordinates ($-13.5, -6, -22.5$), cluster size: 49 voxel with resolution $1.5 \times 1.5 \times 1.5\,mm^3$] (Figure 2B), especially in the left SF amygdala (Figure 2C). In addition, compared with HC group, patients with MDD also showed reduced left SF amygdala volume (Figure 2D).

Changed functional connectivity

Whole brain RSFC analyses identified enhanced functional connectivity strength between the left SF amygdala and left posterior fusiform gyrus in MDD patients after ECT (Figure 3A). Subsequently, we used meta-analysis to define the exact anatomical location of the FFA (Figure 3B) and found a high overlap between the FFA and the identified region showing ECT-induced connectivity changes (Figure 3C). In addition, we found that MDD
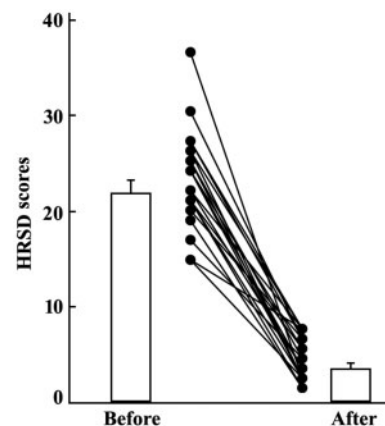

Fig. 1. Mood scores before and after ECT. HRSD was used to assess the level of depression before and after ECT. The mean and SEM HRSD score were shown. A paired two-sided t-test was performed, and a threshold value was set at $P < 0.05$ for significance.
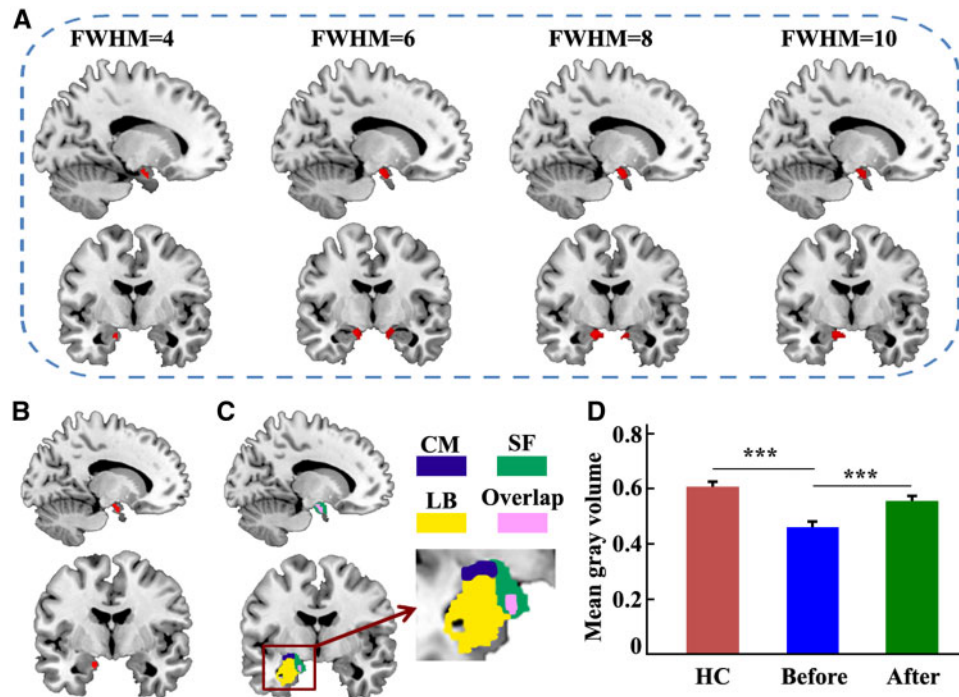
Fig. 2. Longitudinal effect of ECT on amygdala volume. (A) VBM was used to detect the changed GMV. The GMV was smoothed using Gaussian kernels with different FWHM (FWHM = 4, 6, 8 and 10) to identify the consistently changed GMV across different smooth kernels to exclude the effects of different smooth kernels. The whole brain voxel-wise paired *t*-test was used to identify the changed GMV, and FWE method with minimum 30 voxels was used for multicomparison correction ($P < 0.05$, FWE corrected). (B) The consistently increased GMV of left amygdala after ECT was identified by calculating the overlap across different smooth kernels. (C) The changed GMV region was localized by overlapping with the cytoarchitectonic subregions of amygdala including SF amygdala, CM amygdala and LB amygdala. The altered GMV brain area was mainly located on the SF amygdala. (D) The mean GMV of SF amygdala in HC, before ECT and after ECT was calculated. The significantly decreased GMV in MDD patients was identified compared with HC or after ECT. ***$P < 0.001$.
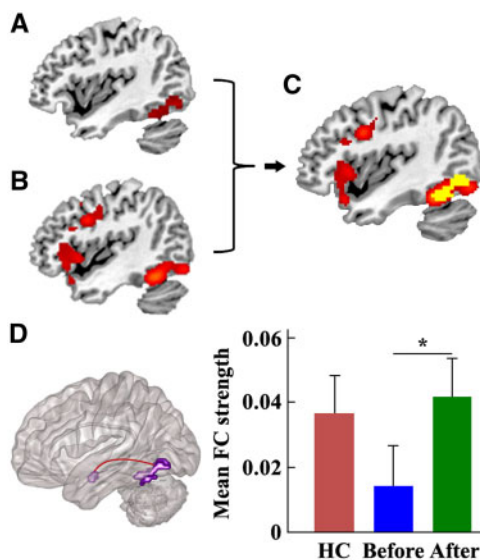

Fig. 3. RSFC analyses of SF subregion of amygdala. (A) Whole brain RSFC analysis of SF subregion was performed, and paired *t*-test was used to reveal the changes of FC. A cluster-level Monte Carlo simulation (5000 times) corrected threshold of $P < 0.05$ was used to identify the significant changes in FC (cluster-forming threshold at voxel-level $P < 0.001$). (B) We used meta-analysis in BrainMap database to define the exact anatomical location of FFA. (C) We overlaid the functionally changed brain area onto the FFA defined using meta-analysis and found the functionally changed brain area was completely overlapped with FFA. (D) The mean FC strength between SF amygdala and FFA in HC, before ECT and after ECT was calculated. The decreased FC in MDD patients was identified. *$P < 0.05$.

patients showed decreased functional connectivity between the left SF amygdala and FFA as compared with HC (Figure 3D).

GCA results

To further determine the causal direction of the effects, a GCA was performed and identified a significant increased magnitude of causal interactions from FFA to amygdala after ECT ($P < 0.05$) (Figure 4). The GCA result indicated that the increased functional connectivity between amygdala and FFA was driven by increasing effects of the FFA on the amygdala.

Classification results

Using the combined features of GMV, RSFC and effective connectivity, the linear SVM classifier achieved an accuracy of 83.33% [82.61% for MDD patients (sensitivity), 84% for HC (specificity)] (Figure 5).

Correlation analyses

Correlation analyses **revealed** that mean GMV in SF amygdala and functional connectivity between SF amygdala and FFA were significantly correlated to symptoms of depression before ECT (Figure 6), which further suggested a direct association between these alterations and depression symptomatology.

Meta-analysis based functional characterization

Behavioral characterization identified a significant association of the left SF amygdala and FFA with cognition memory, visual
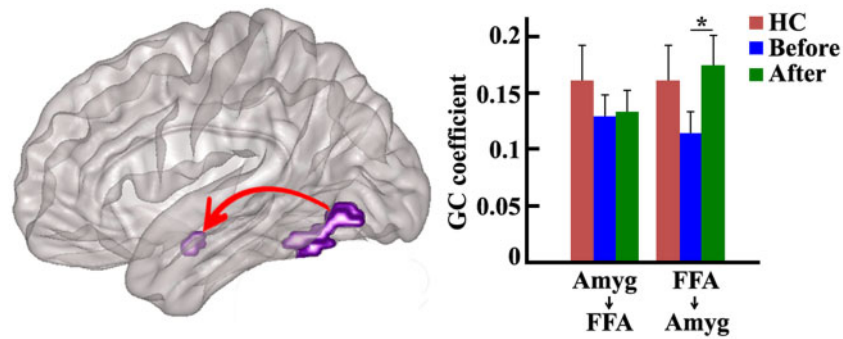
Fig. 4. Effective connectivity between SF amygdala and FFA. GCA was used to calculate the effective connectivity between FFA and SF amygdala in HC, before ECT and after ECT. GCA identified significantly enhanced effective connectivity from FFA to SF amygdala after ECT. Compared with HC, MDD patients showed decreased effective connectivity from FFA to SF amygdala. *$P < 0.05$.
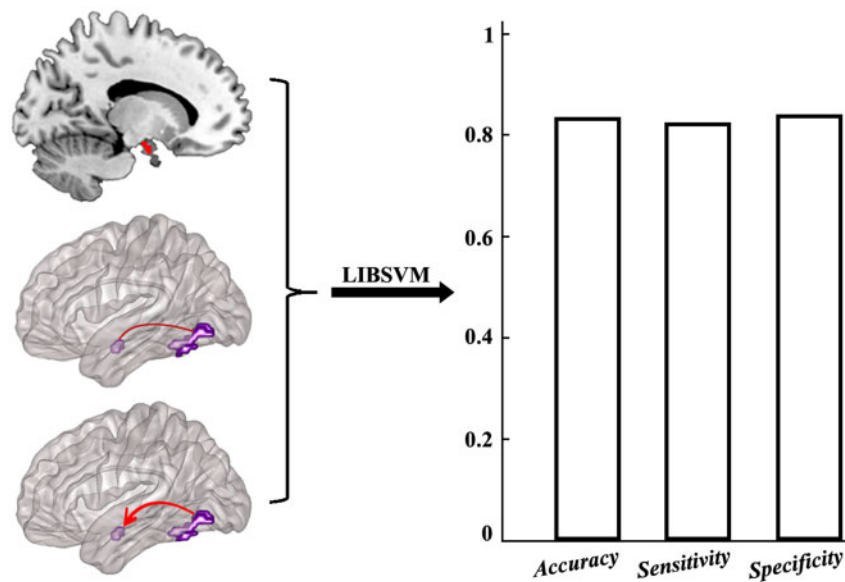

Fig. 5. Multivariate pattern analysis using LIBSVM was applied to provide provisional evidence to determine whether identified neural indices might serve as biomarkers for diagnosing MDD. The regional GMV of amygdala, FC between SF amygdala and FFA and effective connectivity from FFA to SF amygdala were used as the features for classification. We used a leave-one-out cross-validation strategy to estimate the generalization ability of our classifier. The classification accuracy, sensitivity and specificity were showed.

perception, disgust and fear emotion processing and semantic processing (Figure 7).

Discussion

The goal of this study was to explore the possible neuroanatomical basis of ECT improving the clinical response in MDD patients with an average of 2–3 weeks treatment from the first to the last ECT session by establishing the structural and functional changes. VBM and connectivity analyses identified increased GMV of SF nucleus of amygdala, increased RSFC between SF amygdala and FFA and enhanced effective connectivity from FFA to SF amygdala after ECT. Multivariate pattern analysis using linear SVM further demonstrated that these neuroimaging indices can **serve** as a biomarker for diagnosing MDD. These findings indicated that ECT may enhance the neurogenesis of amygdala and the feedforward connection from cortical FFA to subcortical area of SF amygdala to improve the social information processing, early conscious perception of emotion and assessing emotion valence and emotional memory processing in MDD patients.

SF nucleus of amygdala

Amygdala is the core structure for processing of emotion (Zald, 2003), especially for fear processing (Morris *et al.*, 1996), in the brain. Recent studies have indicated that amygdala is a very complex structure composed of a heterogenous group of nuclei and subnuclei, which have distinct cytoarchitectonics (Amunts *et al.*, 2005), functional (Robinson *et al.*, 2010; Bzdok *et al.*, 2013; Mishra *et al.*, 2013) and anatomical connectivity patterns (Bach *et al.*, 2011). Our current findings revealed that ECT mainly increased the volume of the left SF nucleus of amygdala, which was traditionally thought to be exclusively involved in olfactory perception and olfactory-related affective processing (Moreno and Gonzalez, 2007; Bzdok *et al.*, 2013). An increasing number of neuroimaging evidence has suggested that the SF nucleus of amygdala also participated in multiple emotion processing and social information processing (Adolphs, 2008; Hurlemann *et al.*, 2008), and the activity of the SF amygdala can be predicted by the activity of the connected limbic lobe which is the core network for emotion processing (Roy *et al.*, 2009). Recently, using *in vivo* task fMRI, Goossens *et al.* (2009) directly demonstrated that
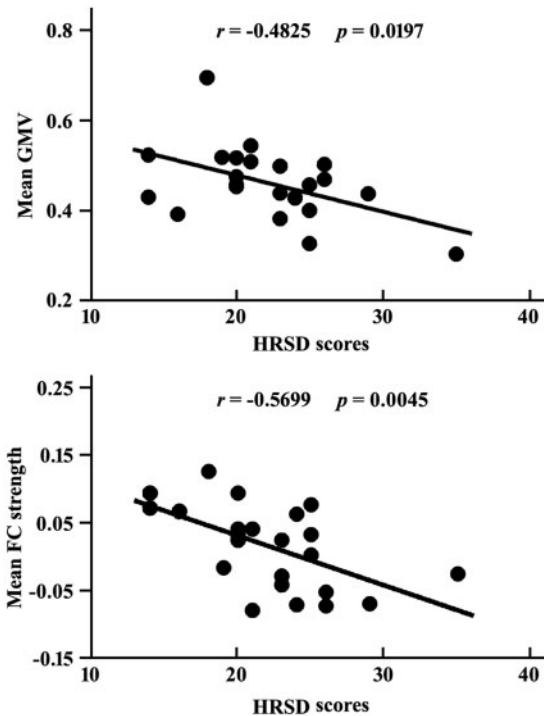
Fig. 6. Correlation analyses between the altered neural indices and HRSD scores. Correlation analyses between the HRSD scores and mean GMV of SF amygdala, mean FC strength between SF amygdala and FFA, mean effective connectivity strength from FFA to SF amygdala were separately performed before and after ECT. The significant correlation between HRSD scores and mean GMV of SF amygdala and mean FC strength before ECT was identified. The significant level was set at $P < 0.05$.
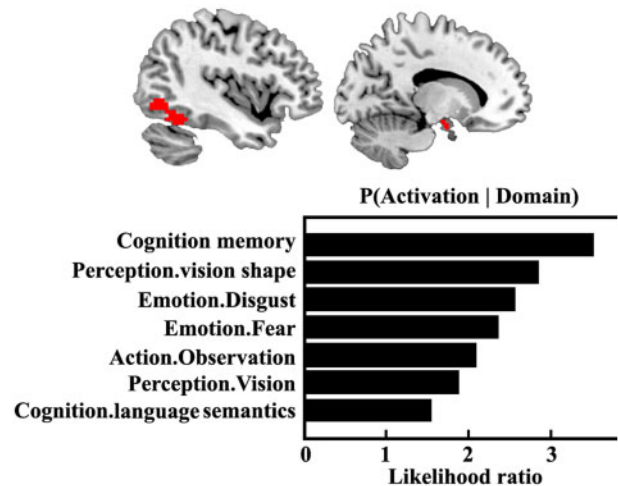

Fig. 7. Behavioral characterization of the significant brain areas of SF amygdala and FFA. Only behavioral domains significantly associated with the FFA and SF amygdala at $P < 0.05$ (FDR corrected) are shown.

SF amygdala selectively extracts the social value of incoming stimuli in human. Therefore, increased GMV of SF amygdala suggested that ECT can improve the emotion processing and social behavior in depression patients. The increased GMV of left amygdala identified in this study was supported by the previous studies which also found increased volume of the left amygdala after ECT (Frodl *et al.*, 2008; Dukart *et al.*, 2014; Joshi *et al.*, 2016) and decreased volume of the amygdala in MDD compared with the HC (Wagner *et al.*, 2008; Depping *et al.*, 2015). Using the same VBM method, Dukart *et al.* (2014) identified increased GMV in hippocampus which actually corresponds to the SF amygdala identified in this study. Additionally, compared with Joshi *et al.*' (2016) findings, we only found increased GMV in SF subregion of amygdala, whereas Joshi *et al.* (2016) additionally found the increased volume of the basolateral (LB) nuclei of amygdala. The difference may result from the heterogeneity of MDD patients and the differences in responses of depression patients after ECT. In a word, our findings, together with previous results, indicated that ECT primarily affects the volume of SF nucleus of amygdala, and the increased volume of amygdala may **serve** as a neuroimaging biomarker for the effect of ECT on depression.

Connectivity between FFA and amygdala

FFA located on the middle fusiform gyrus, a component of the ventral processing stream for visual information and complex feature detection (Kanwisher *et al.*, 1996; Farah and Aguirre, 1999), seems to be specifically involved in the perception of faces and recognition of face identity (Kanwisher *et al.*, 1997; McCarthy *et al.*, 1997). Damage to FFA results in visual agnosia and prosopagnosia (McNeil and Warrington, 1993; Busigny *et al.*,

2010). Given an important role of processing of face information in social interaction, the enhanced functional connectivity between FFA and amygdala identified in this study suggested that ECT may alleviate the symptoms of depression by improving the social abilities to enhance the gaze fixation of face stimuli (Kawashima *et al.*, 1999; Dalton *et al.*, 2005). This claim was supported by previous studies which revealed that SF nucleus of amygdala exclusively participated in complex social judgments of faces (Bzdok *et al.*, 2011) and prosocial value orientation (Haruno and Frith, 2010). Moreover, many previous studies have demonstrated that amygdala plays a key role in early stage processing of facial expression and modulates the sensory processing via back-projections (Breiter *et al.*, 1996; Morris *et al.*, 1998; Zald, 2003). However, using GCA, we found enhanced feedforward connection from FFA to SF nucleus of amygdala not the back-projections from SF nucleus to FFA. The functional modulation of FFA on SF was supported by the direct white matter pathway between the two areas (Catani *et al.*, 2003). Given the fusiform gyrus has been widely reported to take part in processing of novel stimulation for visual features (Koutstaal *et al.*, 2001; Sperling *et al.*, 2001), our findings thus may indicate that ECT could improve the ability of attention to emotional stimuli to facilitate the early conscious perception of emotion and assessing emotional valence (Morris *et al.*, 1998; Groenewold *et al.*, 2013). The meta-analysis of the SF amygdala and FFA revealed that the two areas were primarily involved in cognitive memory (Figure 7). This finding suggested that ECT may also improve the negative emotional or social memory processing in MDD patients (Rock *et al.*, 2014). In addition, since left FFA was overlapped with the visual word form area (VWFA) (Zhang *et al.*, 2016), therefore, FFA enhancing amygdala early conscious perception of emotion and assessing emotion valence may be achieved by verbal processing of emotion stimuli (Morris *et al.*, 1998).

ECT mechanism

There are four main theories were proposed to account for the mechanism of ECT including monoamine neurotransmitter theory, the neuroendocrine theory, the anticonvulsant theory and the neurotrophic theory. The neurotrophic theory which has been widely demonstrated by an increasing number of studies

suggests that ECT can induce neurogenesis and increase neurotrophic signaling (Kellner *et al.*, 2012). Animal models investigations have showed that neurotrophic factor decreased in depressive animal and increased after electroconvulsive shock (Madsen *et al.*, 2000; Hellsten *et al.*, 2002; Wennstrom *et al.*, 2004; Chen *et al.*, 2009; Piccinni *et al.*, 2009). Moreover, neurotrophic factor can modulate limbic circuits to promote treatment-related neuroplasticity including synaptogenesis, gliogenesis, angiogenesis and neurogenesis (Gersner *et al.*, 2010; Eisch and Petrik, 2012; Bouckaert *et al.*, 2014). ECT-mediated neuroplasticity has been replicated in several longitudinal neuroimaging investigations (Dukart *et al.*, 2014; Joshi *et al.*, 2016). In this study, the increased volume of amygdala was found after ECT, which may underlie successful treatment response of depression. Our findings provide the further evidence for the neurotrophic theory of ECT.

Limitations

There are several limitations in this study. First, the numbers of used patients with ECT is small. The larger samples are needed to further validate this findings. Second, the inhomogeneity of the taken medication is also observed in these MDD patients. Thus, to control the medication effects are needed in future study. Third, we used GCA and identified the causal interaction from FFA to SF amygdala indicating that ECT enhanced the top-down modulation of social and emotion processing. However, because of the technical limitation for fMRI acquisition: (i) the sampling rate for fMRI data is usually much slower than the underlying neuronal responses and (ii) fMRI responses reflect convolution with an HRF imposing long delays with respect to neural activity and, even worse, may have significant interregional variability (Seth *et al.*, 2015). Given the GCA of fMRI data is still controversial, thus, our findings using GCA need to be demonstrated with other techniques.

Conclusion

We revealed increased GMV in SF nucleus of amygdala, increased functional connectivity between SF amygdala and FFA and effective connectivity from FFA to SF subregion of amygdala in MDD patients. The following multivariate pattern analysis further demonstrated that the identified neural indices can serve as biomarkers for diagnosing MDD. These findings indicated that ECT can increase the neurogenesis of amygdala to improve the symptoms of depression. In addition, this study also suggested that ECT alleviates depression symptoms by enhancing the feedforward connection from FFA to SF amygdala to improve the negative emotional or social memory processing, and early conscious perception of emotion and assessing emotion valance through verb processing to boost the social behavior. Our findings can facilitate future ECT related clinical researches and help to better understand its mechanism and to diagnose the MDD patients.

Funding

References

Abbott, C.C., Lemke, N.T., Gopal, S., *et al.* (2013). Electroconvulsive therapy response in major depressive disorder: a pilot functional network connectivity resting state FMRI investigation. *Frontiers in Psychiatry*, **4**, 10.

Adolphs, R. (2008). Fear, faces, and the human amygdala. *Current Opinion in Neurobiology*, **18**(2), 166–72.

Amunts, K., Kedo, O., Kindler, M., *et al.* (2005). Cytoarchitectonic mapping of the human amygdala, hippocampal region and entorhinal cortex: intersubject variability and probability maps. *Anatomy and Embryology*, **210**(5–6), 343–52.

Ashburner, J., Friston, K.J. (2000). Voxel-based morphometry–the methods. *Neuroimage*, **11(6 Pt 1)**, 805–21.

Bach, D.R., Behrens, T.E., Garrido, L., Weiskopf, N., Dolan, R.J. (2011). Deep and superficial amygdala nuclei projections revealed in vivo by probabilistic tractography. *Journal of Neuroscience*, **31**(2), 618–23.

Bouckaert, F., Sienaert, P., Obbels, J., *et al.* (2014). ECT: its brain enabling effects: a review of electroconvulsive therapy-induced structural brain plasticity. *The Journal of ECT*, **30**(2), 143–51.

Breiter, H.C., Etcoff, N.L., Whalen, P.J., *et al.* (1996). Response and habituation of the human amygdala during visual processing of facial expression. *Neuron*, **17**(5), 875–87.

Busigny, T., Graf, M., Mayer, E., Rossion, B. (2010). Acquired prosopagnosia as a face-specific disorder: ruling out the general visual similarity account. *Neuropsychologia*, **48**(7), 2051–67.

Bzdok, D., Laird, A.R., Zilles, K., Fox, P.T., Eickhoff, S.B. (2013). An investigation of the structural, connectional, and functional subspecialization in the human amygdala. *Human Brain Mapping*, **34**(12), 3247–66.

Bzdok, D., Langner, R., Caspers, S., *et al.* (2011). ALE meta-analysis on facial judgments of trustworthiness and attractiveness. *Brain Structure & Function*, **215**(3–4), 209–23.

Catani, M., Jones, D.K., Donato, R., Ffytche, D.H. (2003). Occipito-temporal connections in the human brain. *Brain*, **126**(Pt 9), 2093–107.

Chang, C.-C., Lin, C.-J. (2011). LIBSVM: a library for support vector machines. *ACM Transactions on Intelligent Systems and Technology*, **2**(3), 1–27.

Chen, F., Madsen, T.M., Wegener, G., Nyengaard, J.R. (2009). Repeated electroconvulsive seizures increase the total number of synapses in adult male rat hippocampus. *European Neuropsychopharmacology*, **19**(5), 329–38.

Dalton, K.M., Nacewicz, B.M., Johnstone, T., *et al.* (2005). Gaze fixation and the neural circuitry of face processing in autism. *Nature Neuroscience*, **8**(4), 519–26.

Depping, M.S., Wolf, N.D., Vasic, N., Sambataro, F., Thomann, P.A., Christian Wolf, R. (2015). Specificity of abnormal brain volume in major depressive disorder: a comparison with borderline personality disorder. *Journal of Affective Disorders*, **174**, 650–7.

Dukart, J., Regen, F., Kherif, F., *et al.* (2014). Electroconvulsive therapy-induced brain plasticity determines therapeutic outcome in mood disorders. *Proceedings of the National Academy of Sciences of the United States of America*, **111**(3), 1156–61.

Eickhoff, S.B., Stephan, K.E., Mohlberg, H., *et al.* (2005). A new SPM toolbox for combining probabilistic cytoarchitectonic maps and functional imaging data. *Neuroimage*, **25**(4), 1325–35.

Eisch, A.J., Petrik, D. (2012). Depression and hippocampal neurogenesis: a road to remission?. *Science*, **338**(6103), 72–5.

Farah, M.J., Aguirre, G.K. (1999). Imaging visual recognition: PET and fMRI studies of the functional anatomy of human visual recognition. *Trends in Cognitive Sciences*, **3**(5), 179–86.

Ferrari, A.J., Charlson, F.J., Norman, R.E., *et al.* (2013). Burden of depressive disorders by country, sex, age, and year: findings from the global burden of disease study 2010. *PLoS Medicine*, **10**(11), e1001547.

Fox, M.D., Raichle, M.E. (2007). Spontaneous fluctuations in brain activity observed with functional magnetic resonance imaging. *Nature Reviews. Neuroscience*, **8**(9), 700–11.

Frodl, T., Jager, M., Smajstrlova, I., *et al.* (2008). Effect of hippocampal and amygdala volumes on clinical outcomes in major depression: a 3-year prospective magnetic resonance imaging study. *Journal of Psychiatry & Neuroscience*, **33**(5), 423–30.

Gersner, R., Toth, E., Isserles, M., Zangen, A. (2010). Site-specific antidepressant effects of repeated subconvulsive electrical stimulation: potential role of brain-derived neurotrophic factor. *Biological Psychiatry*, **67**(2), 125–32.

Goossens, L., Kukolja, J., Onur, O.A., *et al.* (2009). Selective processing of social stimuli in the superficial amygdala. *Human Brain Mapping*, **30**(10), 3332–8.

Gotts, S.J., Saad, Z.S., Jo, H.J., Wallace, G.L., Cox, R.W., Martin, A. (2013). The perils of global signal regression for group comparisons: a case study of autism spectrum disorders. *Frontiers in Human Neuroscience*, **7**, 356.

Groenewold, N.A., Opmeer, E.M., de Jonge, P., Aleman, A., Costafreda, S.G. (2013). Emotional valence modulates brain functional abnormalities in depression: evidence from a meta-analysis of fMRI studies. *Neuroscience and Biobehavioral Reviews*, **37**(2), 152–63.

Hamilton, J.P., Chen, G., Thomason, M.E., Schwartz, M.E., Gotlib, I.H. (2011). Investigating neural primacy in major depressive disorder: multivariate Granger causality analysis of resting-state fMRI time-series data. *Molecular Psychiatry*, **16**(7), 763–72.

Hamilton, M. (1960). A rating scale for depression. *Journal of Neurology Neurosurgery and Psychiatry*, **23**(1), 56–62.

Haruno, M., Frith, C.D. (2010). Activity in the amygdala elicited by unfair divisions predicts social value orientation. *Nature Neuroscience*, **13**(2), 160–1.

Hellsten, J., Wennstrom, M., Mohapel, P., Ekdahl, C.T., Bengzon, J., Tingstrom, A. (2002). Electroconvulsive seizures increase hippocampal neurogenesis after chronic corticosterone treatment. *The European Journal of Neuroscience*, **16**(2), 283–90.

Hurlemann, R., Rehme, A.K., Diessel, M., *et al.* (2008). Segregating intra-amygdalar responses to dynamic facial emotion with cytoarchitectonic maximum probability maps. *Journal of Neuroscience Methods*, **172**(1), 13–20.

Joshi, S.H., Espinoza, R.T., Pirnia, T., *et al.* (2016). Structural plasticity of the hippocampus and amygdala induced by electroconvulsive therapy in major depression. *Biological Psychiatry*, **79**(4), 282–92.

Kanwisher, N., Chun, M.M., McDermott, J., Ledden, P.J. (1996). Functional imaging of human visual recognition. *Brain Research. Cognitive Brain Research*, **5**(1–2), 55–67.

Kanwisher, N., McDermott, J., Chun, M.M. (1997). The fusiform face area: a module in human extrastriate cortex specialized for face perception. *Journal of Neuroscience*, **17**(11), 4302–11.

Kawashima, R., Sugiura, M., Kato, T., *et al.* (1999). The human amygdala plays an important role in gaze monitoring. A PET study. *Brain*, **122** (Pt 4), 779–83.

Kellner, C.H., Greenberg, R.M., Murrough, J.W., Bryson, E.O., Briggs, M.C., Pasculli, R.M. (2012). ECT in treatment-resistant depression. *The American Journal of Psychiatry*, **169**(12), 1238–44.

Koutstaal, W., Wagner, A.D., Rotte, M., Maril, A., Buckner, R.L., Schacter, D.L. (2001). Perceptual specificity in visual object priming: functional magnetic resonance imaging evidence for a laterality difference in fusiform cortex. *Neuropsychologia*, **39**(2), 184–99.

Lisanby, S.H. (2007). Electroconvulsive therapy for depression. *The New England Journal of Medicine*, **357**(19), 1939–45.

Madsen, T.M., Treschow, A., Bengzon, J., Bolwig, T.G., Lindvall, O., Tingstrom, A. (2000). Increased neurogenesis in a model of electroconvulsive therapy. *Biological Psychiatry*, **47**(12), 1043–9.

McCarthy, G., Puce, A., Gore, J.C., Allison, T. (1997). Face-specific processing in the human fusiform gyrus. *Journal of Cognitive Neuroscience*, **9**(5), 605–10.

McNeil, J.E., Warrington, E.K. (1993). Prosopagnosia: a face-specific disorder. *The Quarterly Journal of Experimental Psychology. Section A*, **46**(1), 1–10.

Mishra, A., Rogers, B.P., Chen, L.M., Gore, J.C. (2013). Functional connectivity-based parcellation of amygdala using self-organized mapping: a data driven approach. *Human Brain Mapping*, **35**(4), 1247–60.

Moreno, N., Gonzalez, A. (2007). Evolution of the amygdaloid complex in vertebrates, with special reference to the anamnio-amniotic transition. *Journal of Anatomy*, **211**(2), 151–63.

Morris, J.S., Frith, C.D., Perrett, D.I., *et al.* (1996). A differential neural response in the human amygdala to fearful and happy facial expressions. *Nature*, **383**(6603), 812–5.

Morris, J.S., Ohman, A., Dolan, R.J. (1998). Conscious and unconscious emotional learning in the human amygdala. *Nature*, **393**(6684), 467–70.

Nobler, M.S., Oquendo, M.A., Kegeles, L.S., *et al.* (2001). Decreased regional brain metabolism after ect. *The American Journal of Psychiatry*, **158**(2), 305–8.

Passingham, R.E., Stephan, K.E., Kotter, R. (2002). The anatomical basis of functional localization in the cortex. *Nature Reviews. Neuroscience*, **3**(8), 606–16.

Perrin, J.S., Merz, S., Bennett, D.M., *et al.* (2012). Electroconvulsive therapy reduces frontal cortical connectivity in severe depressive disorder. *Proceedings of the National Academy of Sciences of the United States of America*, **109**(14), 5464–8.

Piccinni, A., Del Debbio, A., Medda, P., *et al.* (2009). Plasma brain-derived neurotrophic factor in treatment-resistant depressed patients receiving electroconvulsive therapy. *European Neuropsychopharmacology*, **19**(5), 349–55.

Robinson, J.L., Laird, A.R., Glahn, D.C., Lovallo, W.R., Fox, P.T. (2010). Metaanalytic connectivity modeling: delineating the functional connectivity of the human amygdala. *Human Brain Mapping*, **31**(2), 173–84.

Rock, P.L., Roiser, J.P., Riedel, W.J., Blackwell, A.D. (2014). Cognitive impairment in depression: a systematic review and meta-analysis. *Psychological Medicine*, **44**(10), 2029–40.

Roy, A.K., Shehzad, Z., Margulies, D.S., *et al.* (2009). Functional connectivity of the human amygdala using resting state fMRI. *Neuroimage*, **45**(2), 614–26.

Saad, Z.S., Reynolds, R.C., Jo, H.J., *et al.* (2013). Correcting brain-wide correlation differences in resting-state FMRI. *Brain Connectivity*, **3**(4), 339–52.

Santarelli, L., Saxe, M., Gross, C., *et al.* (2003). Requirement of hippocampal neurogenesis for the behavioral effects of antidepressants. *Science*, **301**(5634), 805–9.

Seth, A.K. (2010). A MATLAB toolbox for Granger causal connectivity analysis. *Journal of Neuroscience Methods*, **186**(2), 262–73.

Seth, A.K., Barrett, A.B., Barnett, L. (2015). Granger causality analysis in neuroscience and neuroimaging. *Journal of Neuroscience*, **35**(8), 3293–7.

Sperling, R.A., Bates, J.F., Cocchiarella, A.J., Schacter, D.L., Rosen, B.R., Albert, M.S. (2001). Encoding novel face-name

associations: a functional MRI study. *Human Brain Mapping*, **14**(3), 129–39.

Sridharan, D., Levitin, D.J., Menon, V. (2008). A critical role for the right fronto-insular cortex in switching between central-executive and default-mode networks. *Proceedings of the National Academy of Sciences of the United States of America*, **105**(34), 12569–74.

Wagner, G., Koch, K., Schachtzabel, C., Reichenbach, J.R., Sauer, H., Schlosser, R.G., Md (2008). Enhanced rostral anterior cingulate cortex activation during cognitive control is related to orbitofrontal volume reduction in unipolar depression. *Journal of Psychiatry & Neuroscience*, **33**(3), 199–208.

Wei, Q., Tian, Y., Yu, Y., *et al.* (2014). Modulation of interhemispheric functional coordination in electroconvulsive therapy for depression. *Translational Psychiatry*, **4**, e453.

Wennstrom, M., Hellsten, J., Tingstrom, A. (2004). Electroconvulsive seizures induce proliferation of NG2-expressing glial cells in adult rat amygdala. *Biological Psychiatry*, **55**(5), 464–71.

Zald, D.H. (2003). The human amygdala and the emotional evaluation of sensory stimuli. *Brain Research. Brain Research Reviews*, **41**(1), 88–123.

Zhang, W., Wang, J., Fan, L., *et al.* (2016). Functional organization of the fusiform gyrus revealed with connectivity profiles. *Human Brain Mapping*, **37**(8), 3003–16.